Antiproliferative activity of a series of cisplatin-based Pt(iv)-acetylamido/carboxylato prodrugs

Dalton Transactions

c5dt04905a

1

Antiproliferative activity of a series of cisplatin-based Pt(IV)-acetylamido/carboxylato prodrugs

Mauro Ravera, Elisabetta Gabano, Ilaria Zanellato, Federico Fregonese, Giorgio Pelosi, James A. Platts and Domenico Osella*

The synthesis and biological properties of Pt(IV) complexes exhibiting an asymmetric combination of axial acetylamido and carboxylato ligands are reported.

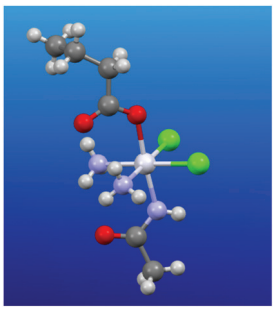

Please check this proof carefully. **Our staff will not read it in detail after you have returned it.**

Translation errors between word-processor files and typesetting systems can occur so the whole proof needs to be read. Please pay particular attention to: tabulated material; equations; numerical data; figures and graphics; and references. If you have not already indicated the corresponding author(s) please mark their name(s) with an asterisk. Please e-mail a list of corrections or the PDF with electronic notes attached – do not change the text within the PDF file or send a revised manuscript. Corrections at this stage should be minor and not involve extensive changes. All corrections must be sent at the same time.

Please bear in mind that minor layout improvements, e.g. in line breaking, table widths and graphic placement, are routinely applied to the final version.

We will publish articles on the web as soon as possible after receiving your corrections; **no late corrections will be made**.

Please return your **final** corrections, where possible within **48 hours** of receipt, by e-mail to: dalton@rsc.org

Queries for the attention of the authors

Journal: **Dalton Transactions**

Paper: **c5dt04905a**

Title: **Antiproliferative activity of a series of cisplatin-based Pt(IV)-acetylamido/carboxylato prodrugs**

Editor's queries are marked like this [Q1, Q2, ...], and for your convenience line numbers are indicated like this [5, 10, 15, ...].

Please ensure that all queries are answered when returning your proof corrections so that publication of your article is not delayed.

Query Reference	Query	Remarks
Q1	For your information: You can cite this article before you receive notification of the page numbers by using the following format: (authors), Dalton Trans., (year), DOI: 10.1039/c5dt04905a.	
Q2	Please carefully check the spelling of all author names. This is important for the correct indexing and future citation of your article. No late corrections can be made.	
Q3	Please check that the inserted CCDC number is correct.	

Dalton Transactions

PAPER

Antiproliferative activity of a series of cisplatin-based Pt(IV)-acetylamido/carboxylato prodrugs†

Cite this: DOI: 10.1039/c5dt04905a

Mauro Ravera,[a] Elisabetta Gabano,[a] Ilaria Zanellato,[a] Federico Fregonese,[a] Giorgio Pelosi,[b] James A. Platts[c] and Domenico Osella*[a]

Received 16th December 2015,
Accepted 2nd February 2016

DOI: 10.1039/c5dt04905a

www.rsc.org/dalton

We report studies of a novel series of Pt(IV) complexes exhibiting an asymmetric combination of acetylamido and carboxylato ligands in the axial positions. We demonstrate efficient synthesis of a series of analogues, differing in the alkyl chain length and hence lipophilicity, from a stable acetylamido/hydroxido complex formed by reaction of cisplatin with peroxyacetimidic acid (PAIA). NMR spectroscopy and X-ray crystallography confirm the identity of the resulting complexes, and highlight subtle differences in the structure and stability of acetylamido complexes compared to the equivalent acetato complexes. Reduction of acetylamido complexes, whether achieved chemically or electro-chemically, is significantly more difficult than that of acetate complexes, resulting in lower antiproliferative activity for shorter-chain complexes. For those with longer chains and hence greater cell uptake, this difference is negated and acetylamido complexes are as active as acetato analogues, both exhibiting antiproliferative potency ($1/IC_{50}$) against A2780 ovarian cancer cells similar to that of cisplatin.

Introduction

Platinum(IV) complexes have been developed in the last decade as a possible alternative to the traditional platinum(II)-based anticancer drugs because of their potential advantages over the latter. Platinum(IV) complexes are quite inert toward ligand substitution and therefore avoid off-target reactions that deactivate Pt(II) complexes and contribute to their side effects. Pt(IV) compounds can reach the tumour site intact, where they are activated through reaction with endogenous reductants, like ascorbate, glutathione or proteins (activation by reduction).[1] Bioreduction of Pt(IV) complexes leads to the corresponding cytotoxic square-planar Pt(II) species by releasing usually both axial ligands. The equatorial ligands determine the nature and activity of the final metabolite, whereas the two axial ligands provide additional opportunities for the tuning of the lipophilicity and the rate of reduction of such Pt(IV) prodrugs.[2,3] Additionally, the axial ligands can play an important role in the drug targeting and delivery (DTD) strategy.[3–6] Pt(IV) derivatives bearing succinic acid/s in the axial position/s are well suited for this purpose, since one carboxylic group is axially linked to the Pt core while the second is available for further reactions with the designed biovectors (active DTD) or with the designed nanoparticles (passive DTD), through amide or ester bonds. Using dihydroxido Pt(IV) synthons for the esterification reaction designed with succinic anhydride, disuccinato Pt(IV) complexes are easily obtained. They can react with one or two designed biovectors often giving mixtures of molecules difficult to be separated, or large aggregates of uncontrolled dimensions in the case of reaction with nanoparticles.[7] Thus, monofunctional (asymmetric) Pt(IV) derivatives are highly desired for such a purpose.[8]

In an attempt to obtain mono-hydroxido Pt(IV) synthons with a chemically inert second axial ligand, the Radziszewski reaction has been recently applied to the synthesis of a new class of Pt(IV) complexes.[9] This method is based on the reaction between acetonitrile and hydrogen peroxide that forms the reactive intermediate peroxyacetimidic acid, PAIA (Scheme 1). PAIA provides a hydroxido and an acetylamido ligand, the latter being *N*-coordinated during the Pt(II) → Pt(IV) oxidation step. The resulting (*OC*-6-44)-(acetylamido-*N*)diamminedichloridohydroxidoplatinum(IV), **1a**, is highly soluble and very stable in water and represents an interesting building block for the further development of Pt(IV) antitumor prodrug candidates. For this purpose, the reactivity of complex **1a** towards different anhydrides and/or activated carboxylic acids has been studied leading to the synthesis of compounds **2a–5a** (Scheme 1). The newly synthesized complexes were tested

[a]*Dipartimento di Scienze e Innovazione Tecnologica, Università del Piemonte Orientale, Viale Teresa Michel 11, 15121 Alessandria, Italy.*
E-mail: domenico.osella@uniupo.it; Fax: +39 0131 360250; Tel: +39 0131 360266
[b]*Dipartimento di Chimica, Università di Parma, Parco Area delle Scienze, 17/A, 43124 Parma, Italy*
[c]*School of Chemistry, Cardiff University, Park Place, Cardiff CF10 3AT, UK*

†Electronic supplementary information (ESI) available: X-ray, water solubility values, redox potentials, HPLC retention times, stability and reduction data of the complexes under investigation. CCDC 1442209. For ESI and crystallographic data in CIF or other electronic format see DOI: 10.1039/c5dt04905a

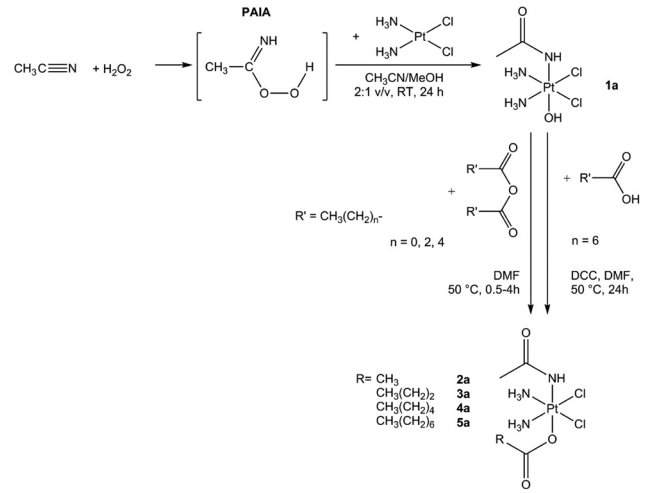

Scheme 1 Reaction scheme for the synthesis of the acetylamido complexes **1a–5a** (DCC = dicyclohexylcarbodiimide).

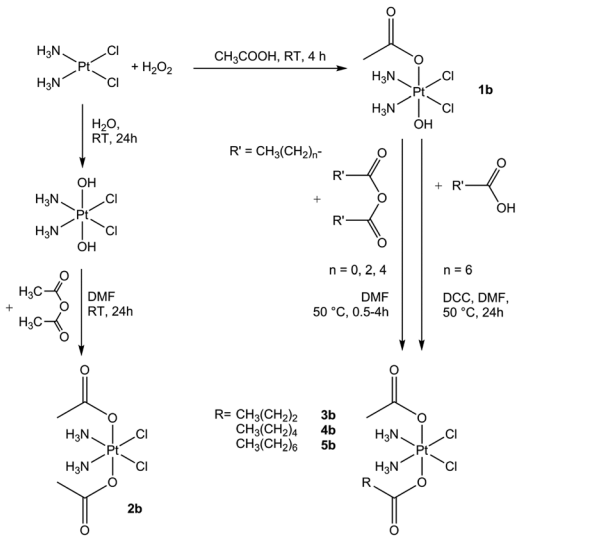

Scheme 2 Reaction scheme for the synthesis of the acetato complexes **1b–5b** (DCC = dicyclohexylcarbodiimide).

in vitro on A2780 ovarian cancer cells. Finally, a series of monoacetato Pt(IV) analogues was added to compare the chemical and biological results (series **b**, Scheme 2).

Experimental section

Materials and methods

$K_2[PtCl_4]$ (Johnson Matthey and Co.) and all other chemicals (Aldrich) were used without further purification. (*SP*-4-2)-Diamminedichloridoplatinum(II) (*i.e.*, cisplatin, *cis*-$[PtCl_2(NH_3)_2]$),[10] (*OC*-6-33)-diacetatodiamminedichloridoplatinum(IV), **2b**,[11] and (*SP*-4-3)-(acetylamido-*N*)diamminechloridoplatinum(II) (*i.e.*, *cis*-$[Pt(acetylamido\text{-}N)Cl(NH_3)_2]$)[12] were synthesized according to literature procedures. The synthesis of **1a** has been recently reported by us,[9] whereas **1b** was synthesized by slight modifications of a previously reported procedure.[13] Complexes **1a** and **1b** were also synthesized using $^{15}NH_3$ to be used in mechanistic studies. All reactions were carried out in aluminum-foil-wrapped vessels.

The purity of the compounds was assessed by analytical RP-HPLC, elemental analysis and determination of the Pt content by inductively coupled plasma-optical emission spectrometry (ICP-OES). Elemental analyses were carried out with an EA3000 CHN Elemental Analyzer (EuroVector, Milano, Italy). Platinum was quantified by means of a Spectro Genesis ICP-OES spectrometer (Spectro Analytical Instruments, Kleve, Germany) equipped with a cross-flow nebulizer. In order to quantify the platinum concentration, the Pt 299.797 nm line was selected. A platinum standard stock solution of 1000 mg L^{-1} was diluted in 1.0% v/v nitric acid to prepare calibration standards.

NMR spectra were recorded on a Bruker Advance III NMR spectrometer operating at 500 (^{1}H), 125.7 (^{13}C), 107.2 (^{195}Pt), and 50.7 MHz (^{15}N), respectively. ^{1}H and ^{13}C NMR chemical shifts were reported in parts per million (ppm) referenced to solvent resonances. ^{195}Pt NMR spectra were recorded using a solution of $K_2[PtCl_4]$ in saturated aqueous KCl as the external reference. The shift for $K_2[PtCl_4]$ was adjusted to −1628 ppm from $Na_2[PtCl_6]$ (δ = 0 ppm). ^{15}N NMR spectra were recorded using a solution of $^{15}NH_4Cl$ in 1 M HCl as the external reference. [^{1}H, ^{15}N] HSQC spectra (Heteronuclear Single Quantum Correlation) were obtained with the standard Bruker sequence hsqcetgpsiz with 0.2 s acquisition time, 8 scans, 1.3 s relaxation delay, and 128 F_1 points. DEPT-45 (Distortionless Enhancement by Polarization Transfer) spectra were recorded with 100 scans, 3.5 s relaxation delay, 0.5 s acquisition time and 75 Hz for ^1J (^{15}N, ^{1}H).

RP-HPLC and mass analysis were performed using a Waters HPLC-MS instrument equipped with the Alliance 2695 separations module, a 2487 dual lambda absorbance detector. The chromatographic conditions were: a silica-based C18 stationary phase (5 μm Phenomenex Phenosphere-NEXT C18 column 250 × 4.6 mm ID), a mobile phase containing 15 mM HCOOH aqueous solution and CH_3OH in different ratios depending on the complex, flow rate = 0.5 mL min^{-1} (isocratic elution), and a UV-visible detector set at 210 nm. Electrospray ionization mass spectra (ESI-MS) were obtained by setting the source and desolvation temperatures to 150 °C and 250 °C, respectively, and using nitrogen both as a drying and a nebulizing gas. The cone and the capillary voltages were usually 30 V or 20 V and 2.70 kV, respectively. The quasi-molecular ion peaks $[M + H]^+$ were assigned on the basis of the *m*/*z* values and of the simulated isotope distribution patterns.

An Autolab PGSTAT12 electrochemical analyser (Eco Chemie, Utrecht, The Netherlands) interfaced to a personal computer running GPES 4.9 electrochemical software was used for the electrochemical measurements. A standard three-electrode cell was designed to allow the tip of the reference electrode (Ag/AgCl, 3 M KCl) to closely approach the working

electrode (a glassy carbon, GC, disk, diameter 0.1 cm, sealed in epoxy resin). The GC working electrode was polished with alumina, then rinsed with distilled water and dried. This process yielded an almost completely reproducible surface for all experiments. All measurements were carried out under nitrogen in ethanol solutions containing 0.1 M $[NBu_4][ClO_4]$ as the supporting electrolyte and the metal complexes 0.50 mM. All potentials are reported *vs.* Ag/AgCl, 3 M KCl. Positive-feedback iR compensation was applied routinely.

Synthesis of complexes 2a–4a. Complex **1a** (100 mg, 0.266 mmol) was suspended in DMF (10 mL) at 50 °C and after 5 min, a 10-fold excess of anhydride (2.66 mmol, *i.e.* 272 mg of acetic anhydride, 422 mg of butyric anhydride, or 570 mg of hexanoic anhydride) was added. The reaction mixture was stirred at 50 °C until the suspension became clear (0.5–4 h). The resulting solution was filtered, the solvent was removed under reduced pressure and the residue was triturated with diethyl ether.

2a. Yield: 111 mg (93%). Elemental analysis: found C, 11.2; H, 3.4; N, 10.3; Pt, 46.5%. Calc. for $C_4H_{13}Cl_2N_3O_3Pt$ C, 11.5; H, 3.1; N, 10.1; Pt, 46.8%. ^{1}H NMR (500 MHz, d_6-DMSO) δ: 1.88 (s, 3H, Pt–O–CO–CH_3), 1.93 (s, 3H, Pt–NH–CO–CH_3), 5.28 (s, 1H, Pt–NH–CO–CH_3), 6.48 (m, 6H, NH_3) ppm. ^{13}C NMR (125.7 MHz, d_6-DMSO) δ: 23.9 (Pt–O–CO–CH$_3$), 24.9 (Pt–NH–CO–CH$_3$), 175.5 (Pt–NH–CO–CH$_3$), 178.3 (Pt–O–CO–CH$_3$) ppm. ^{195}Pt NMR (107.2 MHz, d_6-DMSO) δ: 496 ppm. ESI-MS (positive ion mode): found 418.3 *m*/*z*. Calc. for $[C_4H_{14}Cl_2N_3O_3Pt]^+$ 418.0 *m*/*z* $[M + H]^+$.

3a. Yield: 108 mg (91%). Elemental analysis: found C, 16.0; H, 4.0; N, 9.7; Pt, 44.0%. Calc. for $C_6H_{17}Cl_2N_3O_3Pt$ C, 16.2; H, 3.85; N, 9.4; Pt, 43.8%. ^{1}H NMR (500 MHz, d_6-DMSO) δ: 0.88 (t, J = 7.4 Hz, 3H, Pt–O–CO–CH$_2$–CH$_2$–CH_3), 1.49 (q, J = 7.4 Hz, 2H, Pt–O–CO–CH$_2$–CH_2–CH$_3$), 1.92 (s, 3H, Pt–NH–CO–CH_3), 2.14 (t, J = 7.4 Hz, 2H, Pt–O–CO–CH_2–CH$_2$–CH$_3$), 5.16 (s, 1H, Pt–NH–CO–CH$_3$), 6.48 (m, 6H, NH_3) ppm. ^{13}C NMR (125.7 MHz, d_6-DMSO) δ: 13.8 (Pt–O–CO–CH$_2$–CH$_2$–CH$_3$), 18.9 (Pt–O–CO–CH$_2$–CH$_2$–CH$_3$), 25.1 (Pt–NH–CO–CH$_3$), 38.6 (Pt–O–CO–CH$_2$–CH$_2$–CH$_3$), 175.5 (Pt–NH–CO–CH$_3$), 180.8 (Pt–O–CO–CH$_2$–CH$_2$–CH$_3$) ppm. ^{195}Pt NMR (107.2 MHz, d_6-DMSO) δ: 496 ppm. ESI-MS (positive ion mode): found 446.3 *m*/*z*. Calc. for $[C_6H_{18}Cl_2N_3O_3Pt]^+$ 446.0 *m*/*z* $[M + H]^+$.

4a. Yield: 109 mg (87%). Elemental analysis: found C, 20.0; H, 4.1; N, 8.6; Pt, 41.0%. Calc. for $C_8H_{21}Cl_2N_3O_3Pt$ C, 20.3; H, 4.5; N, 8.9; Pt, 41.2%. ^{1}H NMR (500 MHz, d_6-DMSO) δ: 0.86 (t, J = 6.9 Hz, 3H, Pt–O–CO–CH$_2$–CH$_2$–CH$_2$–CH$_2$–CH_3), 1.26 (m, 4H, Pt–O–CO–CH$_2$–CH$_2$–CH_2–CH_2–CH$_3$), 1.47 (m, 2H, Pt–O–CO–CH$_2$–CH_2–CH$_2$–CH$_2$–CH$_3$), 1.92 (s, 2H, Pt–NH–CO–CH_3), 2.15 (t, J = 7.4 Hz, 2H, Pt–O–CO–CH_2–CH$_2$–CH$_2$–CH$_2$–CH$_3$), 5.16 (s, 1H, Pt–NH–CO–CH$_3$), 6.52 (m, 6H, NH_3) ppm. ^{13}C NMR (125.7 MHz, d_6-DMSO) δ: 13.9 (Pt–O–CO–CH$_2$–CH$_2$–CH$_2$–CH$_2$–CH$_3$), 22.0 (Pt–O–CO–CH$_2$–CH$_2$–CH$_2$–CH$_2$–CH$_3$), 25.1 (Pt–NH–CO–CH$_3$), 25.2 (Pt–O–CO–CH$_2$–CH$_2$–CH$_2$–CH$_2$–CH$_3$), 31.0 (Pt–O–CO–CH$_2$–CH$_2$–CH$_2$–CH$_2$–CH$_3$), 36.6 (Pt–O–CO–CH$_2$–CH$_2$–CH$_2$–CH$_2$–CH$_3$), 175.5 (Pt–NH–CO–CH$_3$), 180.9 (Pt–O–CO–CH$_2$–CH$_2$–CH$_2$–CH$_2$–CH$_3$) ppm. ^{195}Pt NMR (107.2 MHz, d_6-DMSO) δ: 496 ppm. ESI-MS (positive ion mode): found 474.1 *m*/*z*. Calc. for $[C_8H_{22}Cl_2N_3O_3Pt]^+$ 474.1 *m*/*z* $[M + H]^+$.

Synthesis of complex 5a. A solution of *n*-octanoic acid (258 mg, 1.8 mmol) and dicyclohexylcarbodiimide (DCC, 371 mg, 1.8 mmol) in DMF (2 mL) was placed in an ultrasonic bath for 15 min at room temperature. After sonication, the filtered solution was added dropwise to a suspension of **1a** (112 mg, 0.3 mmol) in 2 ml of DMF. The reaction mixture was stirred for 24 h at 50 °C. The solvent was partially removed under reduced pressure and 20 mL of diethyl ether was added to obtain **5a** as a pale yellow powder. Yield: 87 mg (65%). Elemental analysis: found C, 24.4; H, 4.7; N, 8.1; Pt, 39.3%. Calc. for $C_{10}H_{25}Cl_2N_3O_3Pt$ C, 24.0; H, 5.0; N, 8.4; Pt, 39.0%. ^{1}H NMR (500 MHz, d_6-DMSO) δ: 0.86 (t, J = 6.5 Hz, 3H, Pt–O–CO–CH$_2$–CH$_2$–CH$_2$–CH$_2$–CH$_2$–CH$_2$–CH_3), 1.25 (m, 8H, Pt–O–CO–CH$_2$–CH$_2$–CH_2–CH_2–CH_2–CH_2–CH$_3$), 1.46 (m, 2H, Pt–O–CO–CH$_2$–CH_2–CH$_2$–CH$_2$–CH$_2$–CH$_2$–CH$_3$), 1.92 (s, 2H, Pt–NH–CO–CH_3), 2.15 (t, J = 7.5 Hz, 2H, Pt–O–CO–CH_2–CH$_2$–CH$_2$–CH$_2$–CH$_2$–CH$_2$–CH$_3$), 5.16 (s, 1H, Pt–NH–CO–CH$_3$), 6.47 (m, 6H, NH_3) ppm. ^{13}C NMR (125.7 MHz, d_6-DMSO) δ: 13.9 (Pt–O–CO–CH$_2$–CH$_2$–CH$_2$–CH$_2$–CH$_2$–CH$_2$–CH$_3$), 22.1 (Pt–O–CO–CH$_2$–CH$_2$–CH$_2$–CH$_2$–CH$_2$–CH$_2$–CH$_3$), 25.1 (Pt–NH–CO–CH$_3$), 25.5 (Pt–O–CO–CH$_2$–CH$_2$–CH$_2$–CH$_2$–CH$_2$–CH$_2$–CH$_3$), 28.6–28.7 (Pt–O–CO–CH$_2$–CH$_2$–CH$_2$–CH$_2$–CH$_2$–CH$_2$–CH$_3$), 31.2 (Pt–O–CO–CH$_2$–CH$_2$–CH$_2$–CH$_2$–CH$_2$–CH$_2$–CH$_3$), 36.6 (Pt–O–CO–CH$_2$–CH$_2$–CH$_2$–CH$_2$–CH$_2$–CH$_2$–CH$_3$), 175.5 (Pt–NH–CO–CH$_3$), 180.9 (Pt–O–CO–CH$_2$–CH$_2$–CH$_2$–CH$_2$–CH$_2$–CH$_2$–CH$_3$) ppm. ^{195}Pt NMR (107.2 MHz, d_6-DMSO) δ: 496 ppm. ESI-MS (positive ion mode): found 502.2 *m*/*z*. Calc. for $[C_{10}H_{26}Cl_2N_3O_3Pt]^+$ 502.1 *m*/*z* $[M + H]^+$.

Synthesis of complex 1b. Cisplatin (100 mg, 0.33 mmol) was suspended in acetic acid (40 mL) and H_2O_2 50% w/w (1 mL, 35 mmol) was added. The reaction mixture was stirred at room temperature until the solution became clear (*ca*. 3 h). The solution was filtered, the solvent was removed under reduced pressure, and the residue was triturated with diethyl ether to obtain **1b** as a pale yellow solid. Yield: 110 mg (88%). Elemental analysis: found C, 6.6; H, 3.0; N, 7.2; Pt, 51.6%. Calc. for $C_2H_{10}Cl_2N_2O_3Pt$ C, 6.4; H, 2.7; N, 7.45; Pt, 51.9%. ^{1}H NMR (500 MHz, d_6-DMSO) δ: 1.91 (s, 3H, CH_3), 5.93 (t with ^{195}Pt satellites peaks, $^1J_{H-N}$ = 52.9 Hz, $^2J_{H-Pt}$ = 53.0 Hz, 6H, NH_3) ppm. ^{13}C NMR (125.7 MHz, d_6-DMSO) δ: 23.7 (CH_3), 178.4 (Pt–O–CO) ppm. ^{195}Pt NMR (107.2 MHz, d_6-DMSO) δ: 1041 ppm. ESI-MS (positive ion mode): found 377.3 (47%) and 359.0 (100%) *m*/*z*. Calc. for $[C_2H_{11}Cl_2N_2O_3Pt]^+$ 377.0 $[M + H]^+$ and $[C_2H_9Cl_2N_2O_2Pt]^+$ 359.0 $[M - OH]^+$ *m*/*z*.

Synthesis of complexes 3b and 4b. Complex **1b** (100 mg, 0.266 mmol) was suspended in DMF (10 mL) at 50 °C and after 5 min, a 10-fold excess of anhydride (2.66 mmol, *i.e.* 422 mg of butyric anhydride, or 570 mg of hexanoic anhydride or 266 mg of succinic anhydride) was added. The reaction mixture was stirred at 50 °C until the suspension became clear (0.5–4 h). The resulting solution was filtered, the solvent was removed under reduced pressure and the residue was triturated with diethyl ether.

3b. Yield: 106 mg (90%). Elemental analysis: found C, 16.4; H, 3.5; N, 6.5; Pt, 43.4%. Calc. for $C_6H_{16}Cl_2N_2O_4Pt$ C, 16.15; H, 3.6; N, 6.3; Pt, 43.7%. ^{1}H NMR (500 MHz, d_6-DMSO) δ: 0.87 (t, 3H, J = 7.4 Hz, Pt–O–CO–CH_2–CH_2–CH_3), 1.47 (q, 2H, J = 7.4 Hz, Pt–O–CO–CH_2–CH_2–CH_3), 1.90 (s, 3H, Pt–O–CO–CH_3), 2.19 (t, 2H, J = 7.4 Hz, Pt–O–CO–CH_2–CH_2–CH_3), 6.52 (m, 6H, NH_3) ppm. ^{13}C NMR (125.7 MHz, d_6-DMSO) δ: 13.6 (Pt–O–CO–CH_2–CH_2–CH_3), 18.8 (Pt–O–CO–CH_2–CH_2–CH_3), 22.9 (Pt–O–CO–CH_3), 37.7 (Pt–O–CO–CH_2–CH_2–CH_3), 178.2 (Pt–O–CO–CH_3), 180.8 (Pt–O–CO–CH_2–CH_2–CH_3) ppm. ^{195}Pt NMR (107.2 MHz, d_6-DMSO) δ: 1224 ppm. ESI-MS (positive ion mode): found 447.3 m/z. Calc. for $[C_6H_{17}Cl_2N_2O_4Pt]^+$ 447.0 m/z $[M + H]^+$.

4b. Yield: 107 mg (85%). Elemental analysis: found C, 20.0; H, 4.5; N, 5.9; Pt, 41.3%. Calc. for $C_8H_{20}Cl_2N_2O_4Pt$ C, 20.3; H, 4.25; N, 5.9; Pt, 41.1%. ^{1}H NMR (500 MHz, d_6-DMSO) δ: 0.86 (t, J = 7.0 Hz, 3H, Pt–O–CO–CH_2–CH_2–CH_2–CH_2–CH_3), 1.26 (m, 4H, Pt–O–CO–CH_2–CH_2–CH_2–CH_2–CH_3), 1.45 (m, 2H, Pt–O–CO–CH_2–CH_2–CH_2–CH_2–CH_3), 1.90 (s, 2H, Pt–O–CO–CH_3), 2.20 (t, J = 7.4 Hz, 2H, Pt–O–CO–CH_2–CH_2–CH_2–CH_2–CH_3), 6.52 (m, 6H, NH_3) ppm. ^{13}C NMR (125.7 MHz, d_6-DMSO) δ: 13.9 (Pt–O–CO–CH_2–CH_2–CH_2–CH_2–CH_3), 21.9 (Pt–O–CO–CH_2–CH_2–CH_2–CH_2–CH_3), 22.9 (Pt–O–CO–CH_3), 25.1 (Pt–O–CO–CH_2–CH_2–CH_2–CH_2–CH_3), 30.8 (Pt–O–CO–CH_2–CH_2–CH_2–CH_2–CH_3), 35.6 (Pt–O–CO–CH_2–CH_2–CH_2–CH_2–CH_3), 178.2 (Pt–O–CO–CH_3), 180.9 (Pt–O–CO–CH_2–CH_2–CH_2–CH_2–CH_3) ppm. ^{195}Pt NMR (107.2 MHz, d_6-DMSO) δ: 1223 ppm. ESI-MS (positive ion mode): found 475.1 m/z. Calc. for $[C_8H_{21}Cl_2N_2O_4Pt]^+$ 475.0 m/z $[M + H]^+$.

Synthesis of complex 5b. A solution of *n*-octanoic acid (258 mg, 1.8 mmol) and DCC (371 mg, 1.8 mmol) in DMF (2 mL) was placed in an ultrasonic bath for 15 min at room temperature. After sonication, the filtered solution was added dropwise to a suspension of **1b** (113 mg, 0.3 mmol) in 2 ml of DMF. The reaction mixture was stirred for 24 h at 50 °C. The solvent was partially removed under reduced pressure and 20 mL of diethyl ether was added to obtain **5b** as a pale yellow powder. Yield: 82 mg (61%). Elemental analysis: found C, 24.1; H, 5.3; N, 5.5; Pt, 38.9%. Calc. for $C_{10}H_{24}Cl_2N_2O_4Pt$ C, 23.9; H, 4.8; N, 5.6; Pt, 38.8%. ^{1}H NMR (500 MHz, d_6-DMSO) δ: 0.86 (t, J = 6.8 Hz, 3H, Pt–O–CO–CH_2–CH_2–CH_2–CH_2–CH_2–CH_2–CH_3), 1.25 (m, 8H, Pt–O–CO–CH_2–CH_2–CH_2–CH_2–CH_2–CH_2–CH_3), 1.45 (m, 2H, Pt–O–CO–CH_2–CH_2–CH_2–CH_2–CH_2–CH_3), 1.90 (s, 2H, Pt–O–CO–CH_3), 2.20 (t, J = 7.4 Hz, 2H, Pt–O–CO–CH_2–CH_2–CH_2–CH_2–CH_2–CH_2–CH_3), 6.47 (m, 6H, NH_3) ppm. ^{13}C NMR (125.7 MHz, d_6-DMSO) δ: 14.4 (Pt–O–CO–CH_2–CH_2–CH_2–CH_2–CH_2–CH_2–CH_3), 22.6 (Pt–O–CO–CH_2–CH_2–CH_2–CH_2–CH_2–CH_2–CH_3), 23.4 (Pt–O–CO–CH_3), 24.9 (Pt–O–CO–CH_2–CH_2–CH_2–CH_2–CH_2–CH_2–CH_3), 25.8 (Pt–O–CO–CH_2–CH_2–CH_2–CH_2–CH_2–CH_2–CH_3), 29.0 (Pt–O–CO–CH_2–CH_2–CH_2–CH_2–CH_2–CH_2–CH_3), 31.7 (Pt–O–CO–CH_2–CH_2–CH_2–CH_2–CH_2–CH_2–CH_3), 36.2 (Pt–O–CO–CH_2–CH_2–CH_2–CH_2–CH_2–CH_2–CH_3), 178.7 (Pt–O–CO–CH_3), 181.4 (Pt–O–CO–CH_2–CH_2–CH_2–CH_2–CH_2–CH_2–CH_3) ppm. ^{195}Pt NMR (107.2 MHz, d_6-DMSO) δ: 1223 ppm. ESI-MS (positive ion mode): found 503.2 m/z. Calc. for $[C_{10}H_{25}Cl_2N_2O_4Pt]^+$ 503.1 m/z $[M + H]^+$.

Synthesis of $^{15}NH_3$-containing complexes 1a and 1b. The syntheses of complexes **1a** and **1b** containing ^{15}N ammonia were the same as those containing $^{14}NH_3$,[9,13] but started with *cis*-$[PtCl_2(^{15}NH_3)_2]$.[14] The relevant characterization data are reported below.

(^{15}N) 1a. ^{15}N NMR (50.7 MHz, 10% D_2O) δ: −39.7 (with satellite peaks at −37.1 ppm and −42.3 ppm, $^1J_{Pt–N}$ = 260 Hz and $^2J_{Pt–H}$ = 53 Hz) ppm. ^{1}H NMR (500 MHz 10% D_2O) δ: 2.13 (s, 3H, CH_3), 6.11 (d with ^{195}Pt satellite peaks, $^1J_{H–15N}$ = 75 Hz, $^2J_{H–Pt}$ = 53 Hz, 6H, NH_3) ppm. ESI-MS (positive ion mode): found 378.1 (9%) and 360.1 (100%) m/z. Calc. for $[C_2H_{12}Cl_2N^{15}N_2O_2Pt]^+$ 378.0 $[M + H]^+$ and $[C_2H_{10}Cl_2N^{15}N_2OPt]^+$ 360.0 $[M - OH]^+$ m/z.

(^{15}N) 1b. ^{15}N NMR (50.7 MHz, 10% D_2O) δ: −35.7 (with ^{195}Pt satellite peaks at −33.0 ppm and −38.4 ppm, $^1J_{Pt–N}$ = 270 Hz and $^2J_{Pt–H}$ = 53 Hz) ppm; ^{1}H NMR (500 MHz; 10% D_2O) δ: 2.13 (s, 3H, CH_3), 6.06 (d with ^{195}Pt satellite peaks, $^1J_{H–15N}$ = 75 Hz, $^2J_{H–Pt}$ = 53 Hz, 6H, NH_3) ppm. ESI-MS (positive ion mode): found 379.3 (47%) and 361.2 (100%) m/z. Calc. for $[C_2H_{11}Cl_2{}^{15}N_2O_3Pt]^+$ 379.0 $[M + H]^+$ and $[C_2H_9Cl_2{}^{15}N_2O_2Pt]^+$ 361.0 $[M - OH]^+$ m/z.

X-ray structure of 3b

Crystals of **3b** suitable for single-crystal X-ray diffraction were grown by slow evaporation of an aqueous solution of the complex. A specimen of size 0.6 × 0.4 × 0.4 mm, was mounted on a glass fibre and used for data collection on a SMART APEX2 diffractometer [λ(Mo-Kα) = 0.71073 Å]. The crystal is monoclinic, space group $P2_1/c$, cell parameters of a = 10.400 (2), b = 10.093(2), c = 13.361(2) Å, β = 100.644(3)°, V = 1378.4(4) Å^3. The asymmetric unit is formed by two independent molecules of the formula $C_6H_{17}Cl_2N_3O_3Pt$, M_r = 445.21, Z = 4, D_c = 2.14 g cm^{-3}, μ = 10.56 mm^{-1}, F(000) = 840. A semi-empirical absorption correction, based on multiple scanned equivalent reflections, has been carried out and gave 0.3658 < T < 0.7459. A total of 15 205 reflections were collected up to a θ range of 29.31° (±14 h, ± 13 k, ±18 l), 3750 unique reflections (R_{int} = 0.071). The SAINT software[15] was used for the integration of reflection intensity and scaling, and SADABS[16] for the absorption correction. The structures were solved by direct methods using SIR97[17] and refined by full-matrix least-squares on all F^2 using SHELXL97[18] implemented in the WinGX package.[19] All the non-hydrogen atoms in the molecules were refined anisotropically. The hydrogen atoms were partly found and partly placed in the ideal positions using riding models. CCDC 1442209 contains the supplementary crystallographic data (see the ESI†).

Theoretical calculations

DFT calculations were performed at the B3LYP level,[20,21] with the SDD core potential and basis set on Pt[22] and 6-31+G(d,p) on light atoms,[23,24] using Gaussian09.[25] Complexes were built manually and geometry optimised without any symmetry constraint, and the resulting structures were confirmed as true minima through harmonic frequency calculations. Atomic partial charges were calculated using the Natural Bond Orbital

(NBO) scheme.[26] Solvation effects were accounted for by the polarizable continuum model (PCM) approach.[27]

Solution behaviour and reduction reactions

The stability of complexes of the series **a** and **b** was studied by means of ^{1}H NMR spectroscopy. The complexes ([Pt] = 20 mM, except **4a**/**b** and **5a**/**b** where saturated solutions were employed, [Pt] < 20 mM) were dissolved in 100 mM phosphate buffer (D_2O, pH 7.4) and maintained at 25 °C up to 3 d.

The reduction of complexes of the series **a** and **b** (0.5 mM) with ascorbic acid (5 mM) was studied in HEPES (2 mM, pH 7.5) at 25 °C. All these reactions were followed by monitoring the decrease of the area of the chromatographic peaks of the Pt complexes in HPLC-UV-MS. The mobile phase was a mixture of 15 mM aqueous HCOOH and CH_3OH in a ratio depending on the lipophilicity of the complex (from 90/10 to 30/70). ^{15}N NMR spectra of the 20 mM solutions of the Pt complexes and 40 mM ascorbic acid were recorded in 80 mM HEPES with 10% v/v D_2O at 25 °C.

Cell culture and viability tests

The compounds under investigation were tested on the human ovarian carcinoma cell line A2780, from ECACC, purchased from ICLC (Interlab Cell line Collection, IST Genova, Italy). The cells were grown in RPMI-1640 medium supplemented with L-glutamine (2 mM), penicillin (100 IU mL^{-1}), streptomycin (100 mg L^{-1}) and 10% fetal bovine serum. Cell culture and the treatments were carried out at 37 °C in a 5% CO_2 humidified chamber. Cisplatin was dissolved in 0.9% w/v aqueous NaCl solution brought to pH 3 with HCl (final stock concentration 1 mM). All Pt(IV) complexes and [Pt(acetylamido-*N*)Cl(NH_3)$_2$] were dissolved in water or absolute ethanol (final stock concentration 1–5 mM) and stored at −20 °C. The concentration was confirmed by means of ICP-OES.

The mother solutions were diluted in complete medium, to the required concentration range. In the case of co-solvent, the total absolute ethanol concentration never exceeded 0.2% (this concentration was found to be non-toxic to the tested cell). The cells were treated with the compounds under investigation for 72 h. To assess the growth inhibition of the compounds under investigation, a cell viability test, *i.e.* the resazurin reduction assay, was used.[28] Briefly, the cells were seeded in black sterile tissue–culture treated 96-well plates. At the end of the treatment, the viability was assayed by using 10 μg mL^{-1} resazurin (Acros Chemicals, France) in fresh medium for 1 h at 37 °C, and the amount of the reduced product, resorufin, was measured by means of fluorescence (excitation λ = 535 nm, emission λ = 595 nm) with a Tecan Infinite F200Pro plate reader (Tecan, Austria). In each experiment, the cells were challenged with the drug candidates at different concentrations and the final data were calculated from at least three replicates of the same experiment performed in triplicate. The fluorescence of 8 wells containing the medium without cells was used as the blank. The fluorescence data were normalized to 100% cell viability for untreated (NT) cells. The half inhibiting concentration (IC_{50}), defined as the concentration of the drug reducing cell viability by 50%, was obtained from the dose–response sigmoid using Origin Pro (version 8, Microcal Software, Inc., Northampton, MA, USA).

Cellular Pt accumulation

A2780 cells were seeded in 25 cm^2 T-flasks and treated with the complexes under investigations (10 μM) for 4 h. At the end of the exposure, the cells were washed three times with phosphate buffered saline, detached from the Petri dishes using 0.05% Trypsin 1X + 2% EDTA (HyClone, Thermo Fisher) and harvested in fresh complete medium. An automatic cell counting device (Countess®, Life Technologies) was used to measure the number and the mean diameter from every cell count. From the same sample, about 5 × 10^6 cells were taken out for cellular accumulation analysis. Moreover, 100 μL of the medium were taken out from each sample at time zero to check the extracellular Pt concentration. For the cellular Pt accumulation analysis, the cells were transferred into a borosilicate glass tube and centrifuged at 1100 rpm for 5 min at room temperature. The supernatant was carefully removed by aspiration, while about 200 μL of the supernatant were left in order to limit the cellular loss. The cellular pellets were stored at −20 °C until mineralization. Platinum content determination was performed by ICP-MS (Thermo Optek X Series 2). The instrumental settings were optimized in order to yield maximum sensitivity for platinum. For quantitative determination, the most abundant isotopes of platinum and indium (used as the internal standard) were measured at *m*/*z* 195 and 115, respectively. Mineralization was performed by addition of 70% w/w HNO_3 to each sample (after defrosting), followed by incubation for 1 h at 60 °C in an ultrasonic bath. Before the ICP-MS measurement, the HNO_3 was diluted to a final 1% concentration. The cellular Pt accumulation was referred to as ng Pt per 10^6 cells. In order to obtain the Pt cellular concentration, the total cellular volume of each sample was obtained considering the mean cell diameter and cell number estimated by means of an automatic cell counting device (Countess®, Life Technologies). The ratio between the internal and the external cell Pt concentration, namely, the Accumulation Ratio (AR) was computed as previously reported.[29]

Results and discussion

Synthesis of 1a–5a and 1b–5b and X-ray structure of 3a

Complex **1a** has been synthesized upon oxidation of cisplatin with hydrogen peroxide in a mixture of acetonitrile and methanol, according to a recently reported method.[9] During this reaction, the reactive intermediate PAIA (Scheme 1) provides a hydroxide and an acetylamido ligand, the latter being *N*-coordinated during the Pt(II) → Pt(IV) oxidation step. The peroxide PAIA has a quite unstable oxygen–oxygen bond,[30] which should easily split into reactive radicals (namely $^{\bullet}$OH and $^{\bullet}$OC(=NH)CH_3) *via* homolytic cleavage able to coordinate to Pt during its oxidation from the II to the IV redox state. ESR measurements, performed on the reaction mixture using

5,5-dimethyl-1-pyrroline-*N*-oxide (DMPO) as a spin trap, confirm the formation of radical species. However, the presence of several solvents (in particular acetonitrile and methanol that can react with H_2O_2 and change the coupling constants) makes the interpretation of the spectra doubtful.

Interestingly, the final product **1a** has the acetylamido fragment *N*-coordinated. The mesomeric transformation from O-bonded to N-bonded acetylamido is justified considering the relative stability of the two possible complexes. In spite of its high oxidation state, Pt(IV) is classified as a soft ion in Pearson's HSAB theory, and therefore it should prefer N-over O-coordination.[31] Moreover, the ground state energy evaluated for both the isomeric complexes by means of DFT calculations give a free energy difference of 55.8 kJ mol^{-1} in favour of the N-coordinated over the O-coordinated form.

Complex **1b** was obtained from the oxidation of cisplatin with hydrogen peroxide in acetic acid with a slight modification of a previously reported procedure (Scheme 2).[13] These two compounds were reacted with different anhydrides, to obtain the axially asymmetric complexes **2a/b–4a/b**, or with activated *n*-octanoic acid, to obtain **5a** and **5b**. The reaction of **1a** with anhydrides/octanoic acid did not modify the arrangement of the coordinating atoms around the Pt centre (*i.e.* the cisplatin arrangement), as testified by the NMR data. In fact, all complexes of the **a** series show a ^{195}Pt NMR chemical shift similar to that of the prototype **1a**, in the 400–500 ppm region (for series **b** ^{195}Pt NMR chemical shift falls in the 1000–1250 region).

The X-ray structure of **3a**, represented in the ORTEP view of Fig. 1, confirms the presence of a "N_3Cl_2O" arrangement around the Pt atom. The coordination geometry of Pt(IV) is octahedral with the equatorial plane occupied by the two chlorido ligands [Pt–Cl1 2.325(2) and Pt–Cl2 2.314(2) Å] and the two ammonia molecules [Pt–N1 2.052(6) and Pt–N2 2.036(5) Å]. The octahedral coordination is completed by the acetylamido ligand, which occupies one apical position through the deprotonated amino group (Pt–N3 1.987(7) Å), and the butanoato, through the deprotonated OH group (Pt–O2 2.039(6) Å). The arrangement of the axial ligands is very close to linearity (N3–Pt1–O2 175.6(2)°).

The orientation of the butanoato ligand is mainly due to the bifurcated hydrogen bond between its carbonyl and both ammonia molecules. The hydrophobic tail showed a certain degree of disorder and had to be constrained in the refinement. In complex **1a**,[9] the carboxylate plane almost bisected the N–Pt–N angle (47.83°) forming two hydrogen bonds with both ammines, while in this molecule, the acetylamido oxygen is involved in only one intramolecular hydrogen bond with N2 (the corresponding angle is 54.71°). In addition, O1 also forms two intermolecular hydrogen bonds with both ammines of an adjacent centrosymmetrical complex (Fig. 2). Thanks to the latter bonds, the molecules interact pairwise, head-to-tail, forming dimer-like units. These dimeric units are in turn interconnected with each other through another set of hydrogen bonds that involves the butanoate oxygen coordinated to the platinum.

Comparing this molecule with similar ones reported in the literature,[32–34] it is possible to observe a common feature that characterises these structures. When the two equatorial ammines are free to rotate around the Pt–N axis, the oxygen atom of the carbonyl moiety belonging to the ligand in one of

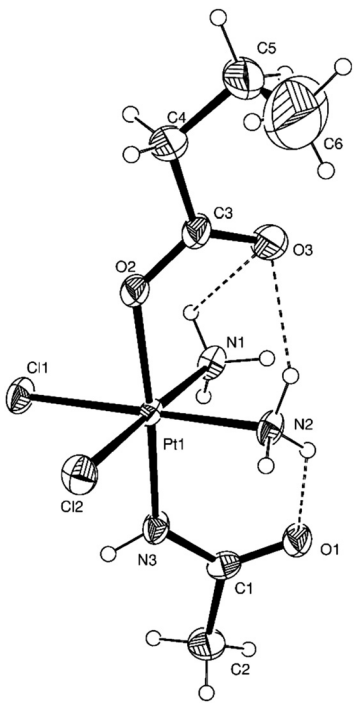

Fig. 1 ORTEP representation of **3a** with ellipsoids at 50% probability (intramolecular hydrogen bonds are represented with dashed lines).

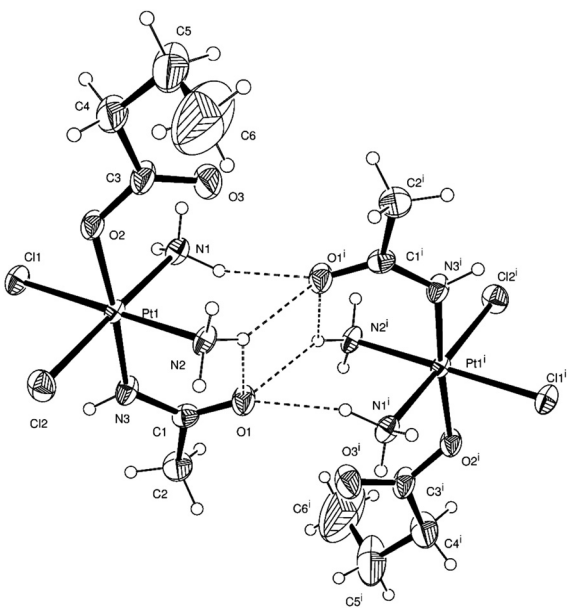

Fig. 2 Scheme of intermolecular hydrogen bonds which contribute to the formation of dimer-like units of two centrosymmetrically related molecules ($i = 1 - x, 1 - y, 1 - z$).

the two axial positions forms a strong bifurcated hydrogen bond with them, orienting their hydrogens. On the opposite side of the coordination plane, the corresponding carbonyl group cannot find ammine hydrogens suitably oriented to form analogous hydrogen bonds and therefore this second carboxyl group is free to rotate around the Pt–O bond and orient itself to form other interactions with neighbouring molecules. In systems in which the ammine groups are part of a more complex molecule,[35] and therefore constrained to certain orientations, the intramolecular hydrogen bonds cannot form and the carboxyl groups are free and involved in single intra- and inter-molecular bonds. To complete the network of interactions that holds together the crystal, an additional hydrogen bond is found between O2 and N2 of an adjacent molecule ($-x + 1, +y + 1/2, -z + 1/2$) which creates a planar network extending parallel to the (100) plane of the unit cell. The hydrophobic tails of the butanoato chains are exposed on both sides of the plane. The whole structure is then completed by van der Waals interactions between the hydrophobic surfaces of these planes (see Fig. S1, ESI†).

Solution behaviour and reduction reactions

The complexes of the two series were kept in phosphate buffer (100 mM in D_2O, pH = 7.4) for 3 d at 37 °C, and the solutions were analysed by means of ^{1}H NMR spectroscopy. The results show that the acetylamido complexes (series **a**) are stable, both when maintained in the dark and exposed to natural daylight cycles (Fig. S2–S6, ESI†), whereas for series **b**, the exposure to light influences the solution behaviour (Fig. S7–S13, ESI†). In fact, all compounds **1b–5b** are stable in the dark (*i.e.*, no variation in the axial acetato ^{1}H NMR peak intensity, taken as diagnostic signal), in the time interval considered (**3d**). In contrast, the methyl signal of **1b** and **2b** decreases with time when the solution is not kept in the dark. After 24 h, the CH_3 peaks of the coordinated acetato ligand decreased by 10 and 20%, for **1b** and **2b**, respectively. At the same time, an increase of the free acetato signal was observed. ^{195}Pt NMR of the aged solutions did not show peaks belonging to Pt(II) derivatives, confirming that hydrolysis, rather than reduction, occurred. It is generally believed that Pt(IV) compounds are quite inert to a ligand substitution reaction; however, it has been reported that aquation reaction may occur to some extent,[36] in particular, after exposure to light or in the presence of residual Pt(II) "impurities" that act as catalysts.[14]

The complexes under investigation were reacted with ascorbic acid (AA) as the simplest model of bio-reductants in order to verify the reduction kinetics and, more importantly, to identify the produced metabolites. All measurements were performed with a 10-fold excess of AA in HEPES buffer, monitoring the decrease of the area of the Pt(IV) HPLC peak. The hydroxido complexes **1a** and **1b** showed a significant decrease of the HPLC peak area (after 24 h **1a** and **1b** showed a decrease in the peak area of about 45% and 60%, respectively) (Fig. S14 and S19, ESI†). In contrast, for all the remaining complexes **2–5**/**a–b**, only a 0–15% of peak decrease was observed in the same timescale (Fig. S5–S18 and S20–S23, ESI†). This is in agreement with the previous observation that the OH ligands favour the kinetics of Pt(IV) reduction over the carboxylato ligands.[37]

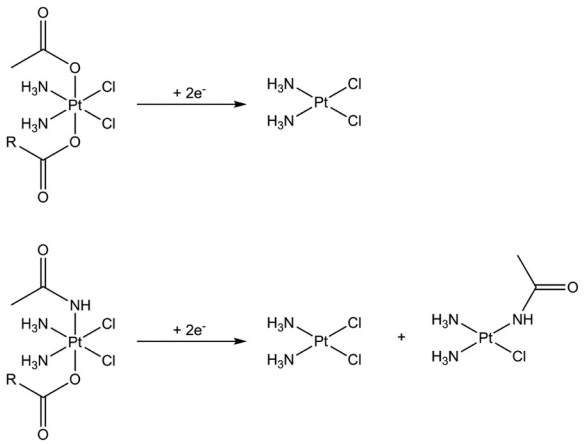

Scheme 3 General reduction scheme of complexes **a** and **b**. Hydrolyzed products and organic residues were omitted for clarity.

As far as the reduction is concerned, the usual Pt(II) metabolites derived from the reductive elimination of the axial ligands (*i.e.*, cisplatin and its hydrolysed derivatives) were observed in both series.[1,11] Interestingly, the reduction process of complexes **a** is also accompanied by the formation of a low quantity of *cis*-[Pt(acetylamido-*N*)Cl(NH_3)$_2$] (Fig. S24, ESI;† ESI-MS shows this complex along with some hydrolyzed species) (Scheme 3).

To confirm these observations, reduction with AA was performed on **1a** and **1b** bearing ^{15}N ammonia[14] as equatorial ligands and followed by ^{15}N NMR (twice excess of AA in HEPES buffer; Fig. S25 and S26, ESI†). After 1 h, the [^{1}H, ^{15}N] HSQC spectra showed the presence of the signals of residual **1a** ($^{15}NH_3$ δ = −39.7 ppm with satellite peaks at −37.1 ppm and −42.3 ppm, $^1J_{Pt-N}$ = 258 Hz and $^2J_{Pt-H}$ = 53 Hz; ^{1}H δ = 6.11 ppm) or **1b** ($^{15}NH_3$ δ = −35.7 ppm with satellite peaks at −33.0 ppm and −38.4 ppm, $^1J_{Pt-N}$ = 270 Hz and $^2J_{Pt-H}$ = 53 Hz; ^{1}H δ = 6.06 ppm), together with that of cisplatin ($^{15}NH_3$ δ = −66.8 ppm with satellite peaks at −63.5 ppm and −69.9 ppm, $^1J_{Pt-N}$ = 327 Hz and $^2J_{Pt-H}$ = 69 Hz; ^{1}H δ = 4.10 ppm). As expected, the signal of cisplatin decreased with time and new peaks appeared at δ = −65.0 ppm (^{1}H δ = 4.33 ppm) and −88.0 ppm (^{1}H δ = 4.25 ppm), respectively. The latter signal falls in the typical region for ^{15}N *trans* to oxygens, supporting the formation of hydrolysed cisplatin.[38]

In the case of **1a**, another peak was present at $^{15}NH_3$ δ = −69.0 ppm (^{1}H δ = 4.33 ppm), in a region common to ^{15}N *trans* to chloridos or nitrogens, compatible with the formation of *cis*-[Pt(acetylamido-*N*)Cl($^{15}NH_3$)$_2$]. Moreover, over time, some other peaks appeared in the region for ^{15}N *trans* to oxygens, indicating the formation of various new hydrolysed species. ^{195}Pt NMR on the same solution showed the signals of cisplatin and its hydrolysed derivative, along with another

peak at −2338 ppm (Fig. S27, ESI†). A genuine sample of *cis*-[Pt(acetylamido-*N*)Cl(NH_3)$_2$][12] showed almost the same ^{195}Pt chemical shift (δ = −2328 ppm in D_2O). Therefore, the combination of NMR and MS information strengthen the hypothesis of the formation of *cis*-[Pt(acetylamido-*N*)Cl(NH_3)$_2$] as a by-product of the reduction of Pt(IV)-acetylamido complexes.

The scrambling between an equatorial chlorido and an axial acetato ligand is not unusual, as clearly showed by Gibson *et al.* following the reduction of a number of Pt(IV) derivatives.[1] The resulting mixed chlorido/carboxylato Pt(II) metabolite should retain the original antiproliferative activity, since Keppler *et al.* demonstrated that monodentate carboxylato ligands bound to Pt(II) complexes are able to undergo efficient activation by aquation.[39] The faster the aquation, the faster the coordination to DNA and the higher the activity. In contrast, the scrambling between an equatorial chlorido and the axial acetylamido ligand, partially occurring during the reduction of **1a**, causes a decrease in the activity of the resulting Pt(II) metabolite, since the *N*-acetylamido ligand cannot easily undergo hydrolysis (see below).

The redox properties of the two series of compounds were tested by linear sweep voltammetry in ethanol solution. All complexes showed the usual Pt(IV)-electrochemical behaviour: a chemically irreversible 2e$^-$, broad reduction peak was observed corresponding to the loss of the two axial ligands and the change from octahedral Pt(IV) to square-planar Pt(II) species.[40] The reduction peak potentials, E_p, of complexes **a** and **b**, reveal that the acetylamido complexes are reduced at a more cathodic potential (ΔE_p = 0.165 V as average difference between the two **a** and **b** series; Table S3, ESI†). The *N*-coordinated acetylamido provides more electronic density on the Pt centre than the acetato counterpart, making the related **a** series (thermodynamically) less easily reducible. This is supported by DFT calculations, from which the atomic partial charge on Pt, calculated using the Natural Bond Orbital (NBO) scheme,[26] in the acetato complex is predicted to be +0.574, compared to that in acetylamido of +0.503. This suggests that *N*-coordination does indeed donate more electron density to Pt than O.

It has been previously reported for cisplatin-, nedaplatin-, picoplatin-, and oxaliplatin-based Pt(IV) complexes that the E_p values measured in water increase (becomes less negative) as the axial chain length increases.[33,41,42] In contrast, it has been observed that in organic solvents, Pt(IV) complexes with different axial chains show very similar E_p values, pointing out that the chain length of the carboxylato ligand has no influence at all on the electronic characteristics of the Pt centre, and, hence, on the reduction potential.[43] In water, different solvation effects on the species involved in the reduction mechanism do influence the final E_p value. The complexes under investigation confirm the latter observation: the E_p values measured in pure ethanol are very similar within each series; unfortunately no well-defined reduction peaks could be observed in water to corroborate the former statement.

Antiproliferative activity

The acetylamido complexes **2a–5a** were tested on ovarian A2780 tumor cells, together with their acetato counterparts **2b–5b**, cisplatin, and *cis*-[Pt(acetylamido-*N*)Cl(NH_3)$_2$] for comparison purposes. The results are expressed in terms of IC_{50} (half-maximal inhibitory concentration) and are reported in Fig. 3 (see also Table S3, ESI†).

It has been reported that Pt(IV) complexes enter cells by passive diffusion only, and unlike cisplatin no influx/efflux mechanism appears to operate.[29] For this reason, lipophilicity, directly related to the ability of a molecule to passively cross cellular membranes, is a key feature to determine the biological activity of such complexes. The lipophilicity of the complexes under investigation was evaluated by means of HPLC, since retention is due to partitioning between the C18 chains of the stationary phase (representing the cellular membrane) and aqueous eluent (representing the water inside and outside cells)[33,44] (Table S3, ESI†). The data show that the retention is minimally affected by the presence of coordinated axial acetato (series **b**) instead of acetylamido (series **a**), whereas it depends mainly on the second axial ligand. As expected, this similarity is reflected on the accumulation ratio (AR) of the **2–5** pairs (Fig. 4, see also Table S3, ESI†). In the literature, uptake and accumulation of Pt are sometimes used as synonymous, but actually the AR is the quotient between the internal and the external cellular Pt concentration. The (internal) cellular Pt concentration is measured taking into account the experimentally measured cell number and average volume of cells; the external Pt concentration is that in the culture medium (experimentally verified by ICP-MS).

In contrast, the acetato complexes **b** show better antiproliferative activity with respect to acetylamido complexes **a** when the companion carboxylato exhibits shorter chains (**2b** and **3b** *vs.* **2a** and **3a**). As the carboxylato ligand chain extends, the antiproliferative activities became quite similar (**4b** and **5b** *vs.* **4a** and **5a**) to the acetylamido ones, matching their similar cell uptake. The difference between **2b–3b** and **2a–3a** may be ascribed to the different kinetics of reduction: the acetato

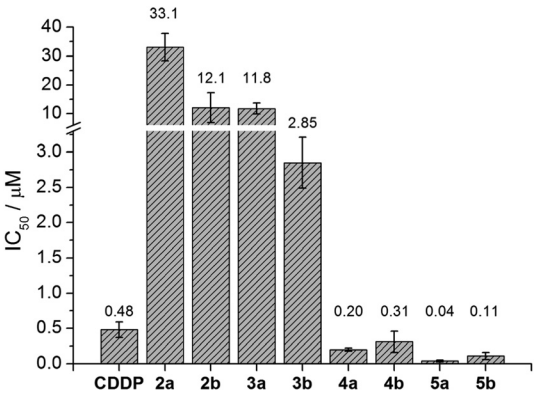

Fig. 3 Half-inhibitory concentration of cisplatin (CDDP), complexes **2a–5a**, and complexes **2b–5b**, measured on A2780 ovarian cancer cells treated for 72 h with the compounds.

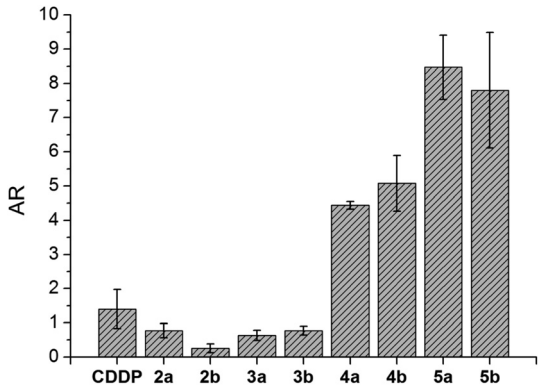

Fig. 4 Accumulation ratio of cisplatin (CDDP), complexes **2a–5a**, and complexes **2b–5b**, measured on A2780 ovarian cancer cells treated for 4 h with the compounds.

series **b** is more prone to reduction than series **a**. Moreover, both series produce cisplatin as the major metabolite, but series **a** produces also a moderate (about 5% in the abiological conditions employed in the reduction experiments with AA) amount of *cis*-[Pt(acetylamido-*N*)Cl(NH_3)$_2$], which is about 50 times less active than cisplatin (IC_{50} = 24.5 μM, measured from a genuine sample). It is well known that monofunctional Pt(II)-triamine complexes such as [PtCl(NH_3)$_3$]$^+$ have lower activity than the bifunctional ones, unless they have a bulky amine, such as phenanthriplatin.[45–48] Thus, the formation of the [Pt(acetylamido-*N*)Cl(NH_3)$_2$] metabolite is detrimental to the overall antiproliferative activity. However, the higher lipophilicity imparted by long chains (**4b–5b** and **4a–5a**) makes the cell uptake so high to mitigate the above differences. Finally, inside each series, the usual relationship is observed: higher lipophilicity corresponds to lower IC_{50}.[42]

Conclusions

A series (**a**) of cisplatin-based asymmetric Pt(IV) complexes of the general formula [Pt(acetylamido-*N*)($CH_3(CH_2)_nCOO$)Cl_2(NH_3)$_2$] (*n* = 0, 2, 4, 6), bearing an acetylamido axial ligand were synthesized and their antiproliferative potential was evaluated. Their cytotoxic activity was investigated in the A2780 ovarian cancer cell line showing IC_{50} values in the low μM range. This antiproliferative activity is similar to or somewhat lower than that of the corresponding acetato series (**b**) [Pt(acetato)($CH_3(CH_2)_nCOO$)Cl_2(NH_3)$_2$] (*n* = 0, 2, 4, and 6) depending on *n*.

Interestingly, starting from *n* = 2, the IC_{50} values are similar to that of the prototype metallo-drug cisplatin. Compounds of series **a** can be obtained easily and in high yield, exhibit an optimal lipophilicity/aqueous solubility balance, and have good stability under light, thus they represent an interesting and promising class of potential antitumor prodrugs.

Acknowledgements

We are indebted to Compagnia di San Paolo (Torino, Italy) for the financial support to the research project BIPLANES. The Inter-University Consortium for Research on the Chemistry of Metals in Biological Systems (CIRCMSB, Bari, Italy), and the UE-COST CM1105 Action "Functional metal complexes that bind to biomolecules" are also acknowledged for providing opportunities for stimulating discussions and short term missions. JAP acknowledges the use of ARCCA (Advanced Research Computing @ Cardiff) facilities for DFT studies.

Notes and references

1 E. Wexselblatt and D. Gibson, *J. Inorg. Biochem.*, 2012, **117**, 220–229.
2 M. D. Hall, H. R. Mellor, R. Callaghan and T. W. Hambley, *J. Med. Chem.*, 2007, **50**, 3403–3411.
3 C. F. Chin, D. Y. Q. Wong, R. Jothibasu and W. H. Ang, *Curr. Top. Med. Chem.*, 2011, **11**, 2602–2612.
4 E. Gabano, M. Ravera and D. Osella, *Curr. Med. Chem.*, 2009, **16**, 4544–4580.
5 J. S. Butler and P. J. Sadler, *Curr. Opin. Chem. Biol.*, 2013, **17**, 175–188.
6 X. Wang, X. Wang and Z. Guo, *Acc. Chem. Res.*, 2015, **48**, 2622–2631.
7 M. Ravera, E. Perin, E. Gabano, I. Zanellato, G. Panzarasa, K. Sparnacci, M. Laus and D. Osella, *J. Inorg. Biochem.*, 2015, **151**, 132–142.
8 M. Ravera, E. Gabano, G. Pelosi, F. Fregonese, S. Tinello and D. Osella, *Inorg. Chem.*, 2014, **53**, 9326–9335.
9 G. Pelosi, M. Ravera, E. Gabano, F. Fregonese and D. Osella, *Chem. Commun.*, 2015, **51**, 8051–8053.
10 S. C. Dhara, *Indian J. Chem.*, 1970, **8**, 193–194.
11 I. Zanellato, I. Bonarrigo, D. Colangelo, E. Gabano, M. Ravera, M. Alessio and D. Osella, *J. Inorg. Biochem.*, 2014, **140**, 219–227.
12 A. Erxleben, I. Mutikainen and B. Lippert, *J. Chem. Soc., Dalton Trans.*, 1994, 3667–3675.
13 J. Z. Zhang, P. Bonnitcha, E. Wexselblatt, A. V. Klein, Y. Najajreh, D. Gibson and T. W. Hambley, *Chem. – Eur. J.*, 2013, **19**, 1672–1676.
14 M. S. Davies, M. D. Hall, S. J. Berners-Price and T. W. Hambley, *Inorg. Chem.*, 2008, **47**, 7673–7680.
15 *SAINT: SAX, Area Detector Integration*, Siemens Analytical Instruments Inc., Madison WI, USA, 1995.
16 G. M. Sheldrick, *SADABS: Siemens Area Detector Absorption Correction Software*, University of Göttingen, Göttingen, Germany, 1996.
17 A. Altomare, M. C. Burla, M. Camalli, G. L. Cascarano, C. Giacovazzo, A. Guagliardi, A. G. G. Moliterni, G. Polidori and R. Spagna, *J. Appl. Crystallogr.*, 1999, **32**, 115–119.
18 G. M. Sheldrick, *Acta Crystallogr., Sect. A: Fundam. Crystallogr.*, 2008, **64**, 112–122.
19 L. Farrugia, *J. Appl. Crystallogr.*, 1999, **32**, 837–838.

20 A. D. Becke, *J. Chem. Phys.*, 1993, **98**, 5648–5652.
21 C. Lee, W. Yang and R. G. Parr, *Phys. Rev. B: Condens. Matter*, 1988, **37**, 785–789.
22 D. Andrae, U. Haussermann, M. Dolg, H. Stoll and H. Preuss, *Theor. Chim. Acta*, 1990, **77**, 123–141.
23 R. Ditchfield, W. J. Hehre and J. A. Pople, *J. Chem. Phys.*, 1971, **54**, 724–728.
24 T. Clark, J. Chandrasekhar, G. W. Spitznagel and P. V. R. Schleyer, *J. Comput. Chem.*, 1983, **4**, 294–301.
25 M. J. Frisch, G. W. Trucks, H. B. Schlegel, G. E. Scuseria, M. A. Robb, J. R. Cheeseman, G. Scalmani, V. Barone, B. Mennucci, G. A. Petersson, H. Nakatsuji, M. Caricato, X. Li, H. P. Hratchian, A. F. Izmaylov, J. Bloino, G. Zheng, J. L. Sonnenberg, M. Hada, M. Ehara, K. Toyota, R. Fukuda, J. Hasegawa, M. Ishida, T. Nakajima, Y. Honda, O. Kitao, H. Nakai, T. Vreven, J. A. Montgomery Jr., J. E. Peralta, F. Ogliaro, M. J. Bearpark, J. Heyd, E. N. Brothers, K. N. Kudin, V. N. Staroverov, R. Kobayashi, J. Normand, K. Raghavachari, A. P. Rendell, J. C. Burant, S. S. Iyengar, J. Tomasi, M. Cossi, N. Rega, N. J. Millam, M. Klene, J. E. Knox, J. B. Cross, V. Bakken, C. Adamo, J. Jaramillo, R. Gomperts, R. E. Stratmann, O. Yazyev, A. J. Austin, R. Cammi, C. Pomelli, J. W. Ochterski, R. L. Martin, K. Morokuma, V. G. Zakrzewski, G. A. Voth, P. Salvador, J. J. Dannenberg, S. Dapprich, A. D. Daniels, Ö. Farkas, J. B. Foresman, J. V. Ortiz, J. Cioslowski and D. J. Fox, *Gaussian 09, Revision D.01*, Gaussian, Inc., Wallingford CT, 2009.
26 A. E. Reed, R. B. Weinstock and F. Weinhold, *J. Chem. Phys.*, 1985, **83**, 735–746.
27 J. Tomasi, B. Mennucci and R. Cammi, *Chem. Rev.*, 2005, **105**, 2999–3093.
28 E. Magnani and E. Bettini, *Brain Res. Protoc.*, 2000, **5**, 266–272.
29 M. Ravera, E. Gabano, I. Zanellato, B. Ilaria, M. Alessio, F. Arnesano, A. Galliani, G. Natile and D. Osella, *J. Inorg. Biochem.*, 2015, **150**, 1–8.
30 R. Benassi and E. Taddei, *Tetrahedron*, 1994, **50**, 4795–4810.
31 S. J. Lippard and J. M. Berg, *Principles of Bioinorganic Chemistry*, University Science Books, 1994.
32 S. Dhar, F. X. Gu, R. Langer, O. C. Farokhzad and S. J. Lippard, *Proc. Natl. Acad. Sci. U. S. A.*, 2008, **105**, 17356–17361.
33 J. A. Platts, G. Ermondi, G. Caron, M. Ravera, E. Gabano, L. Gaviglio, G. Pelosi and D. Osella, *J. Biol. Inorg. Chem.*, 2011, **16**, 361–372.
34 M. Ravera, E. Gabano, S. Bianco, G. Ermondi, G. Caron, M. Vallaro, G. Pelosi, I. Zanellato, I. Bonarrigo, C. Cassino and D. Osella, *Inorg. Chim. Acta*, 2015, **432**, 115–127.
35 V. Gandin, C. Marzano, G. Pelosi, M. Ravera, E. Gabano and D. Osella, *Chemmedchem*, 2014, **9**, 1299–1305.
36 E. Wexselblatt, E. Yavin and D. Gibson, *Angew. Chem., Int. Ed.*, 2013, **52**, 6059–6062.
37 J. Z. Zhang, E. Wexselblatt, T. W. Hambley and D. Gibson, *Chem. Commun.*, 2012, **48**, 847–849.
38 L. Ronconi and P. J. Sadler, *Coord. Chem. Rev.*, 2008, **252**, 2239–2277.
39 D. Hofer, H. P. Varbanov, A. Legin, M. A. Jakupec, A. Roller, M. Galanski and B. K. Keppler, *J. Inorg. Biochem.*, 2015, **153**, 259–271.
40 E. Reisner, V. B. Arion, B. K. Keppler and A. J. L. Pombeiro, *Inorg. Chim. Acta*, 2008, **361**, 1569–1583.
41 M. Ravera, E. Gabano, I. Zanellato, I. Bonarrigo, E. Escribano, V. Moreno, M. Font-Bardia, T. Calvet and D. Osella, *Dalton Trans.*, 2012, **41**, 3313–3320.
42 P. Gramatica, E. Papa, M. Luini, E. Monti, M. B. Gariboldi, M. Ravera, E. Gabano, L. Gaviglio and D. Osella, *J. Biol. Inorg. Chem.*, 2010, **15**, 1157–1169.
43 M. R. Reithofer, A. K. Bytzek, S. M. Valiahdi, C. R. Kowol, M. Groessl, C. G. Hartinger, M. A. Jakupec, M. Galanski and B. K. Keppler, *J. Inorg. Biochem.*, 2011, **105**, 46–51.
44 G. Ermondi, G. Caron, M. Ravera, E. Gabano, S. Bianco, J. A. Platts and D. Osella, *Dalton Trans.*, 2013, **42**, 3482–3489.
45 L. S. Hollis, W. I. Sundquist, J. N. Burstyn, W. J. Heigerbernays, S. F. Bellon, K. J. Ahmed, A. R. Amundsen, E. W. Stern and S. J. Lippard, *Cancer Res.*, 1991, **51**, 1866–1875.
46 L. S. Hollis, A. R. Amundsen and E. W. Stern, *J. Med. Chem.*, 1989, **32**, 128–136.
47 K. S. Lovejoy, R. C. Todd, S. Z. Zhang, M. S. McCormick, J. A. D'Aquino, J. T. Reardon, A. Sancar, K. M. Giacomini and S. J. Lippard, *Proc. Natl. Acad. Sci. U. S. A.*, 2008, **105**, 8902–8907.
48 C. Francisco, S. Gama, F. Mendes, F. Marques, I. C. dos Santos, A. Paulo, I. Santos, J. Coimbra, E. Gabano and M. Ravera, *Dalton Trans.*, 2011, **40**, 5781–5792.